A differential, tilt-independent displacement sensor for the CELT mirror

S. Padin 14 August 2001 rev. 9/11/01

Summary

The capacitive sensors proposed for the CELT mirror are sensitive to vertical displacements of the segments, and also to tilts. The sensitivity to tilt provides some information about the low order mirror modes, but the noise in the active control system is very high for these modes, and it is better to measure them using a wavefront sensor. Using sensors which respond to motions in 2 axes increases the complexity of the calculation required for measuring the high order modes, so it may be advantageous to use sensors that respond only to vertical displacements of the segments. The response of the CELT displacement sensors to segment tilt can be greatly reduced by adding a reference sensor, near each displacement sensor, to measure the tilt. The difference between the displacement and reference sensor outputs is then independent of segment rotation, displacement along the segment edge, inter-segment gap width, and tilting the segment causes just a small sensor gain error, on the order of 0.5 rad^{-1}. If the displacement and reference sensors are close to each other, the differential measurement is highly immune to noise and temperature variations. With a modulation and synchronous detection scheme operating at 1 MHz, and a low-noise differential voltage amplifier at the sensor outputs, the readout noise is < 1 nm in 1 ms.

1. Introduction

The displacement sensors proposed for the CELT mirror segments have a pair of capacitors, made by evaporating metal pads onto the segment edges, as shown in Fig. 1 [1,2]. The sensor capacitances change if a segment is displaced vertically, or tilted, but since the drive pads are wider than the sense pad, the sensor is blind to displacements along the segment edge. The proposed readout for the sensor has a charge amplifier connected to the sense pad, to measure the difference between the two capacitors. This difference depends on the inter-segment gap, which varies with temperature and telescope position. The gap must be measured independently using additional capacitive sensors. The sensor of Fig. 1 also has the disadvantage of a single-ended readout, so a signal from the sense pad (or from the drive circuit) must be transferred across the gap.

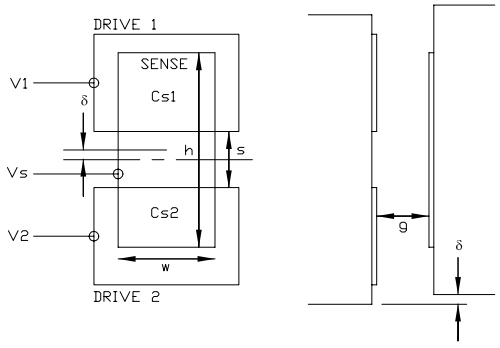

Figure 1: CELT displacement sensor.

2. A gap-independent sensor

The sensitivity of the displacement sensor to gap width can be removed by measuring the voltage, rather than the charge, at the sense pad

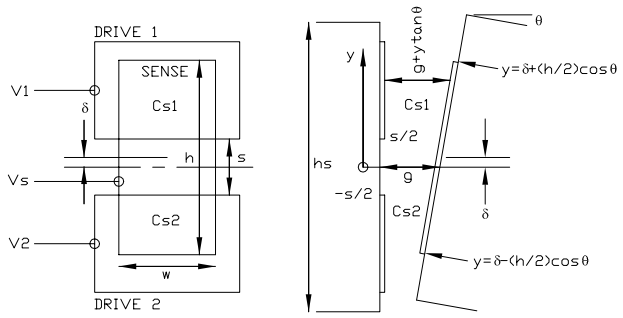

Figure 2: Tilted segment.

$$V_s = V_2 + \frac{(V_1 - V_2)\frac{1}{j\omega C_{s2}}}{\frac{1}{j\omega C_{s1}} + \frac{1}{j\omega C_{s2}}} = V_2 + (V_1 - V_2)\frac{C_{s1}C_{s2}}{C_{s2}(C_{s1}+C_{s2})} = \frac{V_2 C_{s2} + V_1 C_{s1}}{C_{s1}+C_{s2}}$$

If the drive pads are driven differentially, i.e. $V_1 = V$ and $V_2 = -V$, then $V_s = V\frac{C_{s1}-C_{s2}}{C_{s1}+C_{s2}}$

If the inter-segment gap is g and the segment edges are parallel, $C_{s1} = \frac{\epsilon_0 w(\frac{h-s}{2}+\delta)}{g}$ and $C_{s2} = \frac{\epsilon_0 w(\frac{h-s}{2}-\delta)}{g}$, where w and h are the width and height of the sense pad, s is the spacing between the drive pads and δ is the vertical displacement of the segments. Then $V_s = V\frac{2\delta}{h-s}$, which is independent of the width of the gap.

3. A tilt-independent sensor

The displacement sensor in Fig. 1 is sensitive to a tilt of the segment, and the effect is quite large. For a segment tilted through angle θ as in Fig. 2, the inter-segment gap changes by $\Delta g \sim h_s \tan\theta$, over the full height of the segment. The corresponding fractional change in sensor capacitance is $(\frac{\Delta C}{C})_{\Delta g} \sim \frac{\Delta g/2}{g} \sim \frac{h_s \tan\theta}{2g}$, where h_s is the segment height. For the CELT mirror segments, $h_s \sim 50$ mm and $g \sim 2$ mm, so $(\frac{\Delta C}{C})_{\Delta g} \sim 13\tan\theta$. The vertical displacement across the segment due to the tilt is $\delta \sim d_s \sin\theta$, where d_s is the distance across the segment flats. This causes a fractional change in sensor capacitance of $(\frac{\Delta C}{C})_{\delta} \sim \frac{\delta/2}{h_s/2} \sim \frac{d_s \sin\theta}{h_s}$, if the sensor drive pads are about half the height of the segment. With $d_s \sim 0.5$ m, $(\frac{\Delta C}{C})_{\delta} \sim 10\sin\theta$. Since the tilt and displacement responses are similar, it is possible to tilt a segment without substantially changing the output of a sensor on an edge parallel to the tilt axis. The CELT segments will have a displacement sensor near each end of each edge (i.e. 12 sensors per segment). The two sensors on each edge are flipped, so that one end of an edge has a sense pad, and the other end has a pair of drive pads. A tilt about an axis parallel to the edge will change the output of at least one sensor on the edge, but the two sensors may be blind to a combination of tilts. This will not compromise the mirror phasing, because the system is over-determined, but it does increase the complexity of the problem and may impact the time required to achieve a particular surface accuracy.

It is possible to substantially reduce the sensitivity of the displacement sensor to segment tilt, and also provide a differential readout, by adding a reference sensor, as shown in Fig. 3, to measure the tilt. The reference sensor drive pads are bigger than the sense pads, so the sensor is blind to vertical displacements, and to displacements along the segment edge. Since the reference sensor is close to the displacement sensor, and has similar construction, a differential measurement between the two sensors has high immunity to noise and temperature variations.

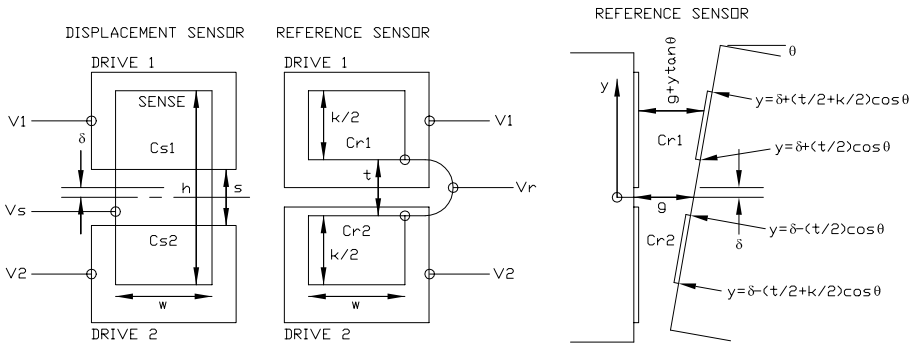

Figure 3: Compensated displacement sensor.

Referring to Fig. 2, for the displacement sensor

$C_{s1} = \int_{\frac{s}{2}}^{\delta+\frac{h}{2}\cos\theta} \frac{\epsilon_0 w}{g+y\tan\theta} dy$ where θ is the tilt of the segment

$= \frac{\epsilon_0 w}{\tan\theta}\left[\ln(g+(\delta+\frac{h}{2}\cos\theta)\tan\theta) - \ln(g+\frac{s}{2}\tan\theta)\right] = \frac{\epsilon_0 w}{\tan\theta}\ln\left[\frac{g+(\delta+\frac{h}{2}\cos\theta)\tan\theta}{g+\frac{s}{2}\tan\theta}\right]$

For $\theta \approx 0$, $C_{s1} \approx \frac{\epsilon_0 w}{\tan\theta}\left[\frac{1}{g}(\delta+\frac{h}{2})\tan\theta - \frac{s}{2g}\tan\theta\right] = \frac{\epsilon_0 w}{g}(\frac{h}{2}+\delta-\frac{s}{2})$, as expected.

$C_{s2} = \int_{\delta-\frac{h}{2}\cos\theta}^{-\frac{s}{2}} \frac{\epsilon_0 w}{g+y\tan\theta} dy = \frac{\epsilon_0 w}{\tan\theta}\ln\left[\frac{g-\frac{s}{2}\tan\theta}{g+(\delta-\frac{h}{2}\cos\theta)\tan\theta}\right]$

and for $\theta \approx 0$, $C_{s2} \approx \frac{\epsilon_0 w}{\tan\theta}\left[-\frac{s}{2g}\tan\theta - \frac{1}{g}(\delta-\frac{h}{2})\tan\theta\right] = \frac{\epsilon_0 w}{g}(\frac{h}{2}-\delta-\frac{s}{2})$, again as expected.

The displacement sensor output is then

$$V_s = V\frac{C_{s1}-C_{s2}}{C_{s1}+C_{s2}} = V\frac{\ln\left[\frac{g+(\delta+\frac{h}{2}\cos\theta)\tan\theta}{g+\frac{s}{2}\tan\theta}\,\frac{g+(\delta-\frac{h}{2}\cos\theta)\tan\theta}{g-\frac{s}{2}\tan\theta}\right]}{\ln\left[\frac{g+(\delta+\frac{h}{2}\cos\theta)\tan\theta}{g+\frac{s}{2}\tan\theta}\,\frac{g-\frac{s}{2}\tan\theta}{g+(\delta-\frac{h}{2}\cos\theta)\tan\theta}\right]}$$

Fig. 4 shows the displacement sensor output, relative to the output with zero tilt, for a sensor with $h = 30$ mm and $s = 10$ mm. (With $V = 10$ V, the sensor gain is 1 V/mm with zero tilt.) For small displacements, the sensitivity to tilt dominates.

Referring to Fig. 3, for the reference sensor

$C_{r1} = \int_{\delta+\frac{t}{2}\cos\theta}^{\delta+(\frac{t}{2}+\frac{k}{2})\cos\theta} \frac{\epsilon_0 w}{g+y\tan\theta} dy = \frac{\epsilon_0 w}{\tan\theta}\ln\left[\frac{g+(\delta+(\frac{t}{2}+\frac{k}{2})\cos\theta)\tan\theta}{g+(\delta+\frac{t}{2}\cos\theta)\tan\theta}\right]$ where $\frac{k}{2}$ is the height of the reference sensor pads and t is the spacing between the pads

$C_{r2} = \int_{\delta-(\frac{t}{2}+\frac{k}{2})\cos\theta}^{\delta-\frac{t}{2}\cos\theta} \frac{\epsilon_0 w}{g+y\tan\theta} dy = \frac{\epsilon_0 w}{\tan\theta}\ln\left[\frac{g+(\delta-\frac{t}{2}\cos\theta)\tan\theta}{g+(\delta-(\frac{t}{2}+\frac{k}{2})\cos\theta)\tan\theta}\right]$

The reference sensor output is

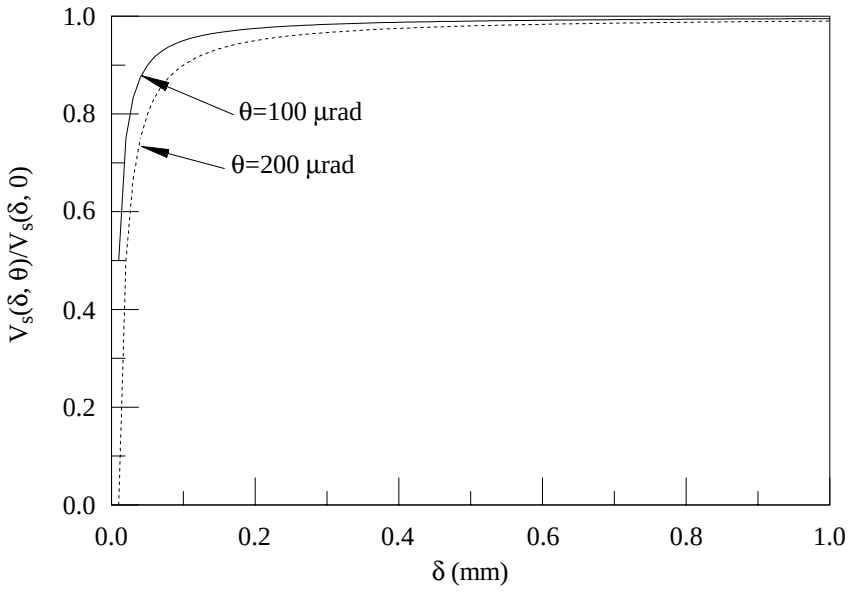

Figure 4: Displacement sensor output relative to the output with zero segment tilt.

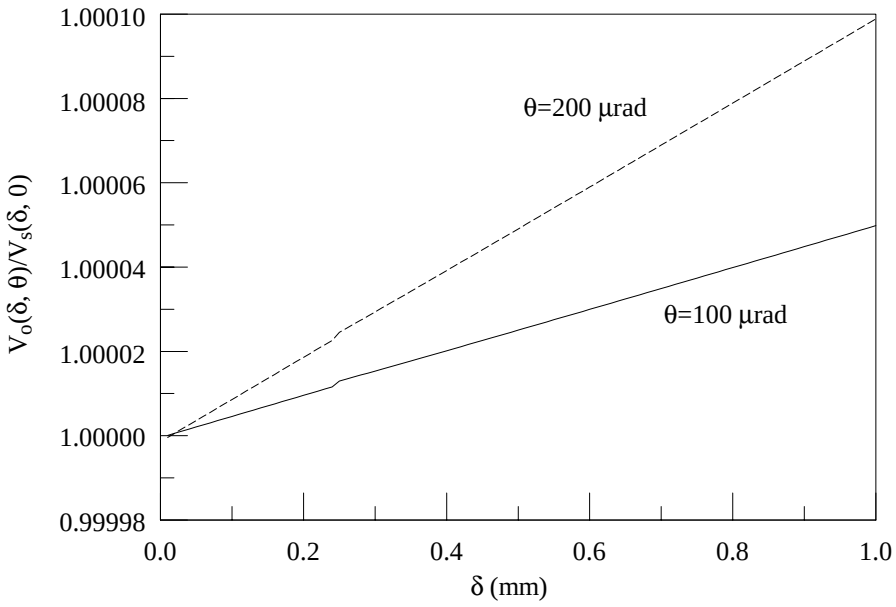

Figure 5: Compensated sensor output relative to the displacement sensor output with zero segment tilt.

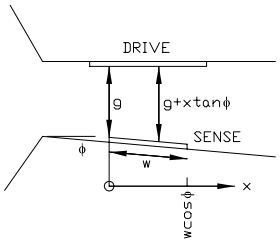

Figure 6: Rotated segment.

$$V_r = V\frac{C_{r1}-C_{r2}}{C_{r1}+C_{r2}} = V\frac{\ln\left[\frac{g+(\delta+(\frac{t}{2}+\frac{k}{2})\cos\theta)\tan\theta}{g+(\delta+\frac{t}{2}\cos\theta)\tan\theta}\,\frac{g+(\delta-(\frac{t}{2}+\frac{k}{2})\cos\theta)\tan\theta}{g+(\delta-\frac{t}{2}\cos\theta)\tan\theta}\right]}{\ln\left[\frac{g+(\delta+(\frac{t}{2}+\frac{k}{2})\cos\theta)\tan\theta}{g+(\delta+\frac{t}{2}\cos\theta)\tan\theta}\,\frac{g+(\delta-\frac{t}{2}\cos\theta)\tan\theta}{g+(\delta-(\frac{t}{2}+\frac{k}{2})\cos\theta)\tan\theta}\right]}$$

Choosing $t+k=h$ and $t=s$ gives $V_r = V_s$ when $\delta = 0$ and $\theta = 0$. Then the output of the compensated sensor is

$$V_o = V_s - V_r = V\frac{\ln\left[\frac{g+(\delta+\frac{h}{2}\cos\theta)\tan\theta}{g+\frac{s}{2}\tan\theta}\,\frac{g+(\delta-\frac{h}{2}\cos\theta)\tan\theta}{g-\frac{s}{2}\tan\theta}\right]}{\ln\left[\frac{g+(\delta+\frac{h}{2}\cos\theta)\tan\theta}{g+\frac{s}{2}\tan\theta}\,\frac{g-\frac{s}{2}\tan\theta}{g+(\delta-\frac{h}{2}\cos\theta)\tan\theta}\right]} - V\frac{\ln\left[\frac{g+(\delta+(\frac{t}{2}+\frac{k}{2})\cos\theta)\tan\theta}{g+(\delta+\frac{t}{2}\cos\theta)\tan\theta}\,\frac{g+(\delta-(\frac{t}{2}+\frac{k}{2})\cos\theta)\tan\theta}{g+(\delta-\frac{t}{2}\cos\theta)\tan\theta}\right]}{\ln\left[\frac{g+(\delta+(\frac{t}{2}+\frac{k}{2})\cos\theta)\tan\theta}{g+(\delta+\frac{t}{2}\cos\theta)\tan\theta}\,\frac{g+(\delta-\frac{t}{2}\cos\theta)\tan\theta}{g+(\delta-(\frac{t}{2}+\frac{k}{2})\cos\theta)\tan\theta}\right]}$$

Fig. 5 shows the compensated sensor output, relative to the output of the displacement sensor with zero tilt, for the same sensor dimensions used for Fig. 4. Tilting the segment just changes the gain of the compensated sensor. This is a much simpler effect than for the uncompensated sensor, and the gain error is only 0.5 rad^{-1} (i.e. 10^{-4} for a 200 μ rad tilt, which corresponds to a displacement of 100 μm across the segment).

4. Segment rotation

From the symmetry of the displacement and tilt sensors, we would expect them to be blind to rotations of the segment in the plane of the mirror surface. From Fig. 6, the displacement sensor capacitances for a segment rotated through angle ϕ are

$$C_{s1} = \int_0^{w\cos\phi}\frac{(\frac{h-s}{2}+\delta)\epsilon_0}{g+x\tan\phi}dx = \frac{(\frac{h-s}{2}+\delta)\epsilon_0}{\tan\phi}[\ln(g+w\cos\phi\tan\phi)-\ln g] = \frac{(\frac{h-s}{2}+\delta)\epsilon_0}{\tan\phi}\ln(1+\frac{w}{g}\cos\phi\tan\phi)$$

$$C_{s2} = \int_0^{w\cos\phi}\frac{(\frac{h-s}{2}-\delta)\epsilon_0}{g+x\tan\phi}dx = \frac{(\frac{h-s}{2}-\delta)\epsilon_0}{\tan\phi}[\ln(g+w\cos\phi\tan\phi)-\ln g] = \frac{(\frac{h-s}{2}-\delta)\epsilon_0}{\tan\phi}\ln(1+\frac{w}{g}\cos\phi\tan\phi)$$

Then, $V_s = V\frac{C_{s1}-C_{s2}}{C_{s1}+C_{s2}} = V\frac{(h-s+2\delta)-(h-s-2\delta)}{(h-s+2\delta)+(h-s-2\delta)} = V\frac{2\delta}{h-s}$ which is independent of ϕ, as expected.

5. Readout electronics

In the scheme of Fig. 3, the readout electronics measures the difference between the displacement and reference sensor output voltages. This avoids transferring a precision signal across the gap, and the drive electronics for a particular sensor can be on a different segment from the readout electronics for that sesnsor. The scheme does require a ground connection between the drive and readout electronics, but this is only to ensure that the signals do not exceed the common mode range of the readout amplifier.

Fig. 7 shows a possible readout circuit for the sensor. In this scheme, the sensor capacitors are

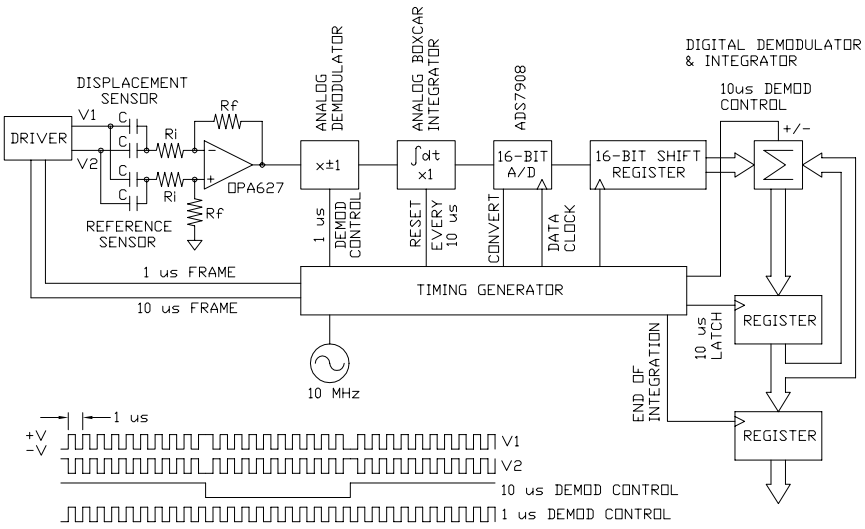

Figure 7: Sensor readout.

driven with complementary square waves. This gives an AC output from the sensor, and demodulation rejects low frequency ($1/f$) noise and offsets in the readout electronics. (Offsets due to fabrication and alignment variations in the sensors would be removed by offsetting the sensor drive, as in the Keck displacement sensors.) Since noise from the readout electronics is rejected for frequencies less than the switching frequency, it is advantageous to switch as fast as possible. This also reduces signal droop due to the finite time constant CR_i. If the switch period is constant, droop is equivalent to reducing the sensor gain, so the effect is a scale-factor error and a reduction in signal-to-noise ratio. With $h = 30$ mm, $s = 10$ mm, $w = 50$ mm and $g = 2$ mm, $C = 2.2$ pF. If $R_i = 1$ MΩ, $CR_i = 2.2$ μs, and a switch period of 1 μs gives 20% signal droop. Larger values of R_i (and hence smaller droop) are possible, but R_f becomes very large because the readout amplifier needs some gain to reduce the noise contribution from subsequent stages. The sensor gain for $h = 30$ mm, $s = 10$ mm and $V = 10$ V is 1 V/mm. With a sensor amplifier gain of 10 and a 16-bit A/D with an input range of ± 1 V, the resolution is 3.1 nm, and the sensor range is ± 100 μm. Displacements outside this range must be handled by reducing the sensor drive voltage (trading range for resolution). With an amplifier gain of 10, $R_f = 10$ MΩ, which is large, but not impractical. The conversion time for inexpensive 16-bit A/Ds is ~ 10 μs, so the readout circuit has a fast analog demodulator, followed by a 10 μs analog boxcar integrator. Offsets in the integrator and A/D are removed by inverting the drive signals every 10 μs and demodulating after the A/D. The demodulated samples are then integrated in a digital integrator to increase the signal-to-noise ratio.

In Fig. 7, the noise spectral density at the sensor output (in V^2/Hz) is

$$V_n^2 = 2e_n^2 + 2R_i^2 i_n^2 + 2(\tfrac{4kT_o}{R_i})R_i^2 + 2(\tfrac{4kT_o}{R_f})R_i^2 + (\tfrac{V_{fs}}{2^n}\tfrac{R_i}{R_f})^2\tau_b$$

where e_n (V/$\sqrt{\text{Hz}}$) and i_n (A/$\sqrt{\text{Hz}}$) are the opamp input noise voltage and current, V_{fs} is the full-scale input range for the A/D, n is the number of bits in the A/D and τ_b is the integration time in the analog boxcar integrator. The first two terms are the opamp input noise [3], the 3rd and 4th terms are Johnson noise from the resistors in the amplifier, and the last term is the quantization noise in the A/D. The fast demodulator rejects noise from the sensor and amplifier at frequencies less than the switching frequency, f_s. Integration for time τ_{int} reduces the noise voltage by a factor $\sim f\tau_{int}$ at frequencies $f \gg 1/\tau_{int}$, so for $f_s \gg 1/\tau_{int}$, the total amplifier noise (in V^2) is $V_{tot}^2 \sim \int_{f_s}^{\infty} \frac{V_n^2}{(f\tau_{int})^2} df$. The opamp

noise voltage and current probably fall as $\sim 1/f$, but for an initial estimate of the noise, assume that all the noise contributions have flat spectra. Then $V_{tot}^2 \sim \frac{V_n^2}{f_s {\tau_{int}}^2}$, so the equivalent bandwidth for the amplifier noise calculation is $\frac{1}{f_s {\tau_{int}}^2}$. For $f_s = 1$ MHz and $\tau_{int} = 1$ ms, $\frac{1}{f_s {\tau_{int}}^2} = 1$ Hz. Demodulation in the digital part of the system rejects A/D noise at frequencies less than $1/\tau_b$, which is 10 times smaller than f_s in the scheme of Fig. 7. The equivalent bandwidth for the A/D noise calculation is $\frac{\tau_b}{{\tau_{int}}^2}$, and for $\tau_b = 10$ μs and $\tau_{int} = 1$ ms, $\frac{\tau_b}{{\tau_{int}}^2} = 10$ Hz. The various noise contributions, referred to the sensor input are

				total noise
	V^2/Hz		nV/$\sqrt{\text{Hz}}$	nV
opamp noise voltage (at 10 kHz)	$2e_n^2$	$e_n = 6$ nV/$\sqrt{\text{Hz}}$	8.5	8.5
opamp noise current (at 100 Hz)	$2R_i^2 i_n^2$	$R_i = 1$ MΩ, $i_n = 2.5$ fA/$\sqrt{\text{Hz}}$	3.5	3.5
Johnson noise in resistors R_i	2 x $4kT_oR_i$	$R_i = 1$ MΩ, $T_o = 290$ K	178.9	178.9
Johnson noise in resistors R_f	2 x $(\frac{4kT_o}{R_f})R_i^2$	$R_f = 10$ MΩ, $T_o = 290$ K	56.6	56.6
A/D quantization noise	$(\frac{V_{fs}}{2^n}\frac{R_i}{R_f})^2\tau_b$	$V_{fs} = 2$ V, $\tau_b = 10$ μs, $n = 16$	9.7	30.5
				190.3

The amplifier voltage and current noises are from the Burr-Brown OPA627 data sheet. These values are for too low a frequency, so the amplifier noise estimate is an upper limit. The total noise for 1 ms integration time is 190 nV, which corresponds to a displacement of 0.2 nm. The noise is dominated by Johnson noise in the amplifier resistors. This could be reduced by increasing the switching frequency, f_s, which would permit smaller values of R_i and R_f without increasing the signal droop. At higher switch frequencies, slew rates in the amplifier and demodulator may be a problem, and the noise immunity of the sensor will decrease because its pads are quite large. Note that the simple analysis presented here does not include noise contributions from the analog demodulator and boxcar integrator, but these should be small because the sensor amplifier has a gain of 10, and low frequency noise is rejected by the 10 μs switching. The A/D noise contribution may be optimistic for an inexpensive A/D, and $n = 13$ might be a more realistic estimate of the equivalent number of bits. In this case the A/D noise contribution would be ~ 90 nV.

The readout circuit in Fig. 7 looks fairly complicated, but each sensor requires just 3 opamps (1 package), an A/D and a digital integrator. The digital parts of the system, including the interface to a computer, could be realized in a field-programmable gate array on each segment. This would allow reconfiguration of the driver, synchronous detector and integrator via the computer interface. The circuit requires some timing signals, which could be distributed to each segment along with the computer interface, possibly using the same cables. It is probably an advantage to have all sensors synchronized, since this permits blanking the analog integrators during drive transitions. If pickup of globally distributed drive signals is a problem, a more complicated modulation scheme may be required (e.g. orthogonal Walsh functions driving different parts of the mirror). A reasonable design goal would be to support each segment with a single simple connection (e.g. a phone jack, or maybe a pair of fibers and a power cable).

References

[1] T.S. Mast and J.E. Nelson, "Segmented Mirror Control System Hardware for CELT, Proceedings of the SPIE, 4003, 2000

[2] G. Chanan, J.E. Nelson, C. Ohara and E. Sirko, Design Issues for the Active Control System of the California Extremely Large Telescope, Proceedings of the SPIE, 4004, 2000

[3] P. Horowitz and W. Hill, The Art of Electronics, (Cambridge: Cambridge University Press) p. 447